Physical Review & Research International
3(2): 137-144, 2013

SCIENCEDOMAIN *international*
www.sciencedomain.org

Simulation of Nanostructures Fabricated in Chalcogenide Glasses for use as Surface-enhanced Raman Scattering Substrates

A. Zakery[1*], A. Asrar[1] and S. R. Elliott[2]

[1]Department of Physics, College of Science, Shiraz University, Shiraz 71454, Iran.
[2]Department of Chemistry, Cambridge University, Cambridge CB2 1EW, UK.

Authors' contributions

This work was carried out in collaboration between all authors. Author AZ designed the study, wrote the first and final drafts of the manuscript. Author AA managed the literature searches and performed simulations. Author SRE. provided experimental details and helped in writing of the final draft. All authors read and approved the final manuscript.

Research Article

Received 5th December 2012
Accepted 5th March 2013
Published 19th March 2013

ABSTRACT

We have simulated the Chalcogenide glass (ChG)-based nanostructures which are used as substrates for surface-enhanced Raman scattering (SERS). A discrete dipole approximation method was used and calculated results are compared to those of experimental. The results of simulation agreed well with the experiment. Furthermore, we have obtained conditions under which higher enhancement factors (almost by an order of magnitude) could be achieved by changing the polarization state and the incident angle of the beam on the surface.

Keywords: SERS; Chalcogenide.

1. INTRODUCTION

It has been almost 40 years since it was recognized that the Raman spectra of sub monolayer coverage of molecules could be acquired on electrochemically roughened coinage metal (Silver) surfaces [1-4]. Since then, the field of surface enhanced Raman spectroscopy (SERS) has grown dramatically, demonstrating its power as an analytical tool

[*]Corresponding author: Email: zakeri@susc.ac.ir;

for the sensitive and selective detection of molecules adsorbed on noble metal nanostructures.

Understanding the mechanisms of SERS has been a struggle since the early days of its inception, when the primary goal was merely explaining the 10^6-fold intensity enhancement of the normal Raman scattering cross-section. At the time, the enhancement factor, $EF_{SERS} = 10^6$, could be understood as the product of two contributions: (a) an electromagnetic enhancement mechanism and (b) a chemical enhancement mechanism. These two mechanisms arise because the intensity of Raman scattering is directly proportional to the square of the induced dipole moment, μ_{ind}, which, in turn, is the product of the Raman polarizability, α, and the magnitude of the incident electromagnetic field, E. As a consequence of exciting the localized surface Plasmon resonance (LSPR) of a nanostructured or nanoparticle metal surface, the local electromagnetic field is enhanced by a factor of 10, for example. Because Raman scattering approximately scales as E^4, the electromagnetic enhancement factor is of order 10^4. Researchers viewed the chemical enhancement factor of 10^2 as arising from the excitation of adsorbate localized electronic resonances or metal-to-adsorbate charge-transfer resonances (e.g., resonance Raman scattering). It is also worthwhile to note that surface-enhanced resonance Raman scattering with combined SERS and resonance Raman scattering enhancement factors in the 10^9–10^{10} range was possible at the time. Despite this enhancement, which made SERS orders of magnitude more sensitive than normal Raman spectroscopy, the full power of SERS unfortunately was not utilized until this past decade. Early systems suffered immensely from irreproducibility owing to ill-defined substrates fabricated by electrochemical roughening [2].

Recent advances in nanofabrication and the 1997 discovery of single-molecule SERS [5,6], the ultimate limit of detection, have caused an explosion of new research and the extension of SERS from an interesting physical phenomenon to a robust and effective analytical technique. In addition, surface preparation and modification techniques [7-10] have also allowed for analyte selectivity.

The need for new SERS-based sensing, detecting, and monitoring platforms has also driven new instrumental techniques such as the integration of SERS active substrates into fiber-optic assemblies [11]. Su et al. report a new technique in their recent articles [12,13]. In the first Letter, they presented what they believed to be a new class of SERS substrates based on chalcogenide glasses (ChGs). Owing to their photosensitivity, periodic nanostructures can be easily fabricated in ChG thin films in a convenient and cost effective way. By coating with a thin Au layer, such nanostructures act as effective SERS substrates and are capable of producing detectable Raman signals for low concentrations of analyte molecules. Experiments with aqueous Rhodamine 6G (R6G) solutions were conducted to investigate the behavior of ChG-based nanostructures as SERS substrates. In their work the performance of these SERS substrates is compared with that of silver nanoparticles made using a citrate reduction method. The potential of their SERS substrate for quantitative analysis, as well as its reproducibility, is discussed in some detail. We simulated their experiment using a discrete dipole approximation method and obtained results which will be discussed in further detail.

2. DISCRETE DIPOLE APPROXIMATION METHOD

The Discrete dipole approximation [14] (DDA) starts by dividing the object of interest into a cubic array of *N*-point dipoles whose positions are denoted by $\boldsymbol{r}_i$, with polarizabilities $\boldsymbol{\alpha}_i$.

The polarization induced in each dipole as a result of interaction with a local electric field $\boldsymbol{E}_{loc}$ will be (omitting the frequency factors $e^{i\omega t}$),

$$\boldsymbol{P}_i = \boldsymbol{\alpha}_i . \boldsymbol{E}_{loc}(\boldsymbol{r}_i) \tag{1}$$

$\boldsymbol{E}_{loc}$, for isolated particles, is the sum of an incident field and a contribution from all other dipoles in the same particle,

$$\boldsymbol{E}_{loc}(\boldsymbol{r}_i) = \boldsymbol{E}_{loc,i} = \boldsymbol{E}_{inc,i} + \boldsymbol{E}_{self,i} = \boldsymbol{E}_0 \exp(i\boldsymbol{K}.\boldsymbol{r}_i) - \sum_{j\neq i} \boldsymbol{A}_{ij}.\boldsymbol{P}_j \tag{2}$$

$\boldsymbol{E}_0$ and $\boldsymbol{K}$ are the amplitude and wave vector of the incident wave, respectively, and the interaction matrix $\boldsymbol{A}$ has the following form:

$$\boldsymbol{A}_{ij}.\boldsymbol{P}_j = \frac{e^{ikr_{ij}}}{r_{ij}^3}\left\{K^2 \boldsymbol{r}_{ij} \times \left(\boldsymbol{r}_{ij} \times \boldsymbol{P}_j\right) + \frac{(1-ikr_{ij})}{r_{ij}^2} \times [r_{ij}\boldsymbol{P}_j - 3\boldsymbol{r}_{ij}(\boldsymbol{r}_{ij}.\boldsymbol{P}_j)]\right\} \quad , \quad (j \neq i) \tag{3}$$

where $K = \omega / c$. Substituting Eq. (2) into Eq. (1) and rearranging terms in the equation, we generate an equation of the form

$$\boldsymbol{A}'.\boldsymbol{P} = \boldsymbol{E} \tag{4}$$

Where $\boldsymbol{A}'$ is a matrix which is built out of the matrix $\boldsymbol{A}$ from Eq. (3) and all dots after $\boldsymbol{A}$, $\boldsymbol{A}'$ and $\boldsymbol{\alpha}$ denote matrix multiplication whereas they denote vector dot products in other cases. For a system with a total of *N* dipoles, $\boldsymbol{E}$ and $\boldsymbol{P}$ in Eq. (4) are 3*N*-dimensional vectors, and $\boldsymbol{A}'$ is a 3*N*×3*N* matrix. By solving these 3*N* complex linear equations, polarization vectors are obtained, and with these, optical cross sections, local fields and the Raman enhancement factor can be calculated.

As noted earlier we used the DDA for simulating the desired experiments [12]. The SERS substrate composed of near semicircular dots (with a diameter d=460 nm) and intervening holes as seen in the SEM image. In the atomic force microscope (AFM) image, the semicircular dots in the SEM images appeared to be hemispheres with a height of 70 nm (Fig. 1).

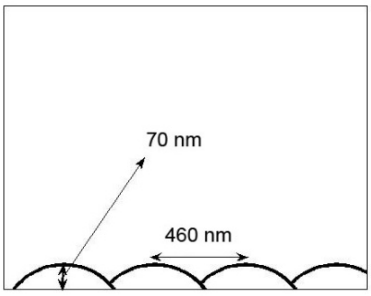

Fig. 1. Simulated SERS substrate.

The SERS substrate used composed of overlapped hemispheres which produced nanoparticles with a volume of the order of 10^7 (nm) ^{3}. It is shown [14] that DDA is suitable

for particles of the same order of volume (e. g. spheroids with major axis 200 nm and aspect ratio 2:1).

We divided each nanoparticle (each hemisphere) into 2116 cubes where each cube showed one dipole. Because of the rapidly decreasing of EF with distance, practically none of the neighboring cube had a significant effect in our calculations. So we considered only the effect of the first neighboring cube in our calculations. We calculated EF for three different polarizations and eleven different incident angles. We assumed that R6G molecules were distributed uniformly on the surface. For calculation of the number of R6G molecules adsorbed on surface with different concentrations, it is clear that Avogadro's number (A) of molecules exist in one liter of solution in one-molar solution. So $\mathrm{A}^{2/3}$ of molecules exist on $(10 \times 10)\ \mathrm{cm}^2$ of surface and hence is the calculated number of molecules adsorbed (exist) on our desired surface. DDA method will be more accurate by a correct choice of polarizability $\boldsymbol{\alpha}_i$ in eq. (1) as was used in [15]. Due to a lack of reliable data on dielectric constants of gold nanoparticles of desired size we used dielectric constants of smaller gold nanoparticles which were reported in [16], and obtained good results.

3. RESULTS AND DISCUSSIONS

In this simulation we obtained EF=1.478×10^6 for a vertical incident beam which is one order greater than that of the usual silver nanoparticle substrates [12]. Relative intensities are in good agreement with experimental results [12] (Fig. 2).

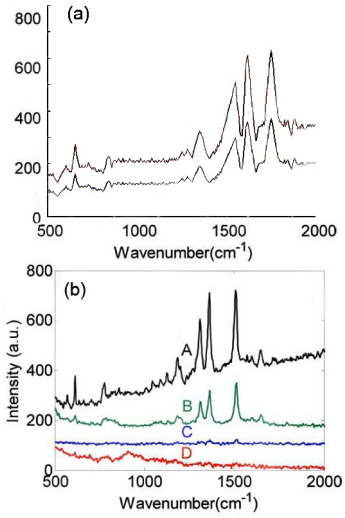

Fig. 2a. The top plot is simulated SERS substrate signal and the lower one is simulated Raman spectra of Ag nanoparticles which correspond to A and B in (b) respectively, (b) : Experimental R6G Raman spectra obtained [12] with A, SERS substrates at 50 mW (0.28 kW/cm^2) and 100 µM concentration; B, silver nanoparticles at 500 mW (2.8 kW/cm^2) and 1 mM concentration; C, silver nanoparticles at 50 mW (0.28 kW/cm^2) and 1mM concentration; D, smooth Au surface at 500 mW (2.8 kW/cm^2) and 1 mM concentration

By choosing the wave-number position of Raman peaks we found the relative intensity for the two substrates (sers and silver nanoparticle substrates). We calculated the number of

R6G molecules on the surface of a nanoparticle. For 1, 10, 50 and100 μM we obtained 13, 60, 249 and 390 molecules respectively. In this case intensities are proportional to the number of molecules on each nanoparticle; (Fig. 3).

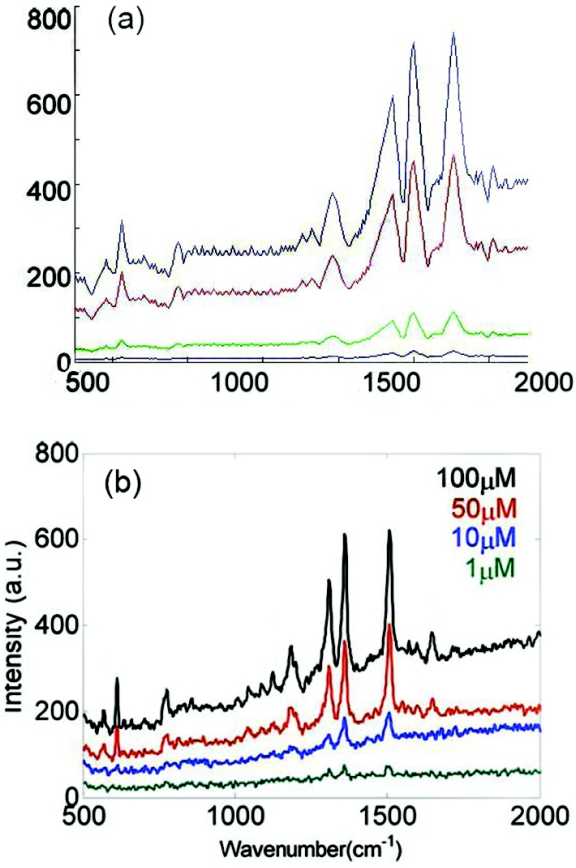

Fig. 3a. Simulation of detected SERS signals for different concentrations of R6G solution, (b) Detected SERS signals at different R6G concentrations with an excitation of 50 mW (0.28 kW/cm^2) [12]

We also calculated EF for 11 different angles equally spaced in range 0- 90º and for different polarizations. A result obtained for three different polarizations is shown in Fig. 4 (angles are in radian). Although the state of the polarization was known at the incidence (in the experiment) but its state was not known after passing through various optical elements before being detected. The free space incident beam angle in [13] was 90 degrees. But we obtained conditions that EF can be larger than that reported in [13].

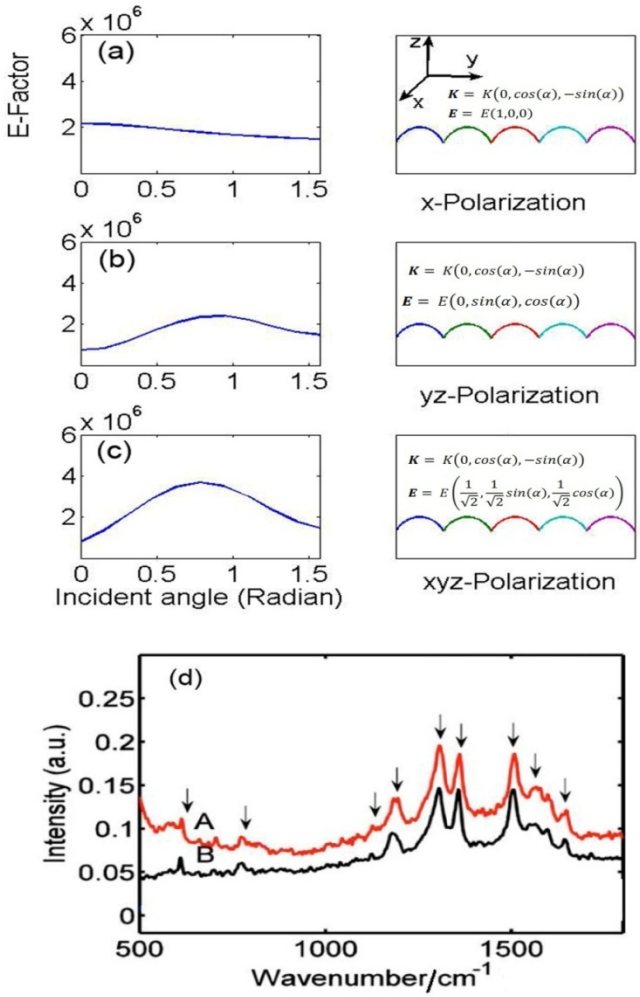

Fig. 4a. Simulation of enhancement factor versus the incident angle for x-polarization; (b) : for yz polarization; (c) : for xyz polarization; (d) Raman spectra obtained [13] with A, fiber-taper-coupled SERS substrate; B, conventional free-space laser-focusing method

For example in Fig. 4 for xyz-polarization and incident beam that makes an angle of $\pi/4$ with the surface, the free space EF is four times greater than parallel radiation (with surface) which is like the case of an evanescent wave. So we suggest some situations rather than evanescent wave that give higher EF than that of [13]; see Fig. 4. Relative intensity between evanescent wave and free space wave in [13] is approximately 4/3 which is roughly obtained for x-polarization in our simulations. Other two polarizations do not yield the same result. As seen in Fig. 4, although for x-polarization we have the largest EF for the case of zero angle incidence (evanescent wave), for other polarizations EF is a maximum near π/4.

Some errors in our work are because of (perhaps) inexact dielectric constant of gold nanoparticles. Results with better agreement can be achieved by considering more dipoles in our calculations.

4. CONCLUSION

In summary, the results of our simulation of ChG-based nanostructures compared well with those of experimental. Moreover, we have obtained conditions under which higher enhancement factors (almost by an order of magnitude) could be achieved by changing the polarization state and the incident angle of the beam on the surface. These ChG-based substrates are compatible with ChG photonic circuits [17] to form integrated SERS sensor chips.

ACKNOWLEDGEMENT

A. Z. would like to thank Shiraz University for a Sabbatical leave.

COMPETING INTERESTS

Authors have declared that no competing interests exist.

REFERENCES

1. Fleischmann M, Hendra PJ, Mc Quillan AJ, Raman spectra of Pyridine adsorbed at a silver electrode, Chemical Physics letters. 1974;26(2):163-166.
2. Stiles PL, Dieringer JA, Shah NC, Van Duyne RP. Surface enhanced Raman spectroscopy, Annu. Rev. Anal. Chem. 2008;1:601.
3. Jeanmarie DI, Van Duyne RP. Surface Raman spectro electrochemistry, part 1: heterocyclic, aromatic, and aliphatic amines adsorbed on the anodized silver electrode, J. Electroanal. Chem. 1977;1:84.
4. Albrecht MG, Creighton JA. Anomalously intense Raman spectra of pyridine at a silver electrode, J. Am. Chem. Soc. 1977;99:5215.
5. Nie SM, Emery SR. Probing single molecules and single nanoparticles by surface-enhanced Raman scattering, Science. 1997;275:1102.
6. Kneipp K, Wang Y , Kneipp H, Perelman LT, Itzkan I. Single molecule detection using surface-enhanced Raman scattering (SERS), Phys. Rev. Lett. 1997;78:1667.
7. Dick LA, McFarland AD, Haynes CL, Van Duyne RP. Metal film over nanosphere (MFON) electrodes for surface-enhanced Raman spectroscopy (SERS): improvements in surface nanostructure stability and suppression of irreversible loss, J. Phys. Chem. B. 2002;106:853.
8. Jensen TR, Malinsky MD, Haynes CL, Van Duyne RP. Nanosphere lithography: tunable localized surface plasmon resonance spectra of silver nanoparticles, J. Phys. Chem. B. 2000;104:10549.
9. Malinsky MD, Kelly KL, Schatz GC, Van Duyne RP. Nanosphere lithography: effect of substrate on the localized surface plasmon resonance spectrum of silver nanoparticles, J. Phys. Chem. B. 2001;105:234.
10. Zhang X, Zhao J, Whitney A, Elam J, Van Duyne RP. Ultrastable substrates for surface-enhanced Raman spectroscopy fabricated by atomic layer deposition: improved anthrax biomarker detection, J. Am. Chem. Soc. 2006;128:10304.
11. Stokes DL, Alarie JP, Ananthanarayanan V, Vo-Dinh T. Fiber optic SERS sensor for environmental monitoring, Proc. SPIE. 1999;3534:647.
12. Su L, Rowlands CJ, Elliott SR. Nanostructures fabricated in Chalcogenide glass for use as surface-enhanced Raman scattering substrates, Opt. Lett. 2009;34:1645.

13. Su L, Rowlands CJ, Elliott SR. Evanecent Wave excitation of surface enhanced Raman scattering substrates by optical fiber taper, Opt. Lett. 2009;34:2685.
14. Yang WH, Schatz GC, Van Duyne RP. Discrete dipole approximation for calculating optical absorption spectra and surface-enhanced Raman intensities for adsorbates on metal nanoparticles with arbitrary shapes, J. Chem. Phys. 1995;103:869.
15. Draine BT, Goodman J. Beyond Clausius-Mossotti Wave propagation on a polarizable point lattice and the discrete dipole approximation, Astrophys. J. 1993;405:685.
16. Stoller P, Jacobsen V, Sandoghdar V. Measurement of the complex dielectric constant of a single gold nanoparticle, Opt. Lett . 2006;31:2474.
17. Ta'eed V, Shokooh-Saremi M, Fu L, Moss DJ, Rochette M, Littler ICM, Eggleton BJ, Ruan YL, Luther-Davies B. Integrated all-optical pulse regenerator in chalcogenide waveguides, Opt. Lett. 2005;30:2900.

Peer-review history:
The peer review history for this paper can be accessed here:
http://www.sciencedomain.org/review-history.php?iid=201&id=4&aid=1124